FAST PLASMA STREAMS RECORDED NEAR THE EARTH DURING 1985–1996

H. MAVROMICHALAKI and A. VASSILAKI
Nuclear and Particle Physics Section, Physics Department, University of Athens, Panepistimioupolis, Ilissia, 15771 Athens, Greece;
E-mail: emavromi@atlas.uoa.gr

(Received 23 August 1997; accepted 18 June 1998)

Abstract. A reference catalogue of 373 well-defined high-speed plasma streams identified in the solar wind measurements from 1985 to 1996 is reported. The data base for this study is the interplanetary plasma/magnetic field data compilation made available by the NSSDC/WDC-A for rockets and satellites (NASA/GSFC-Greenbelt). The main characteristics of those streams, such as the beginning time, the duration, the origin of them (corotating or flare-generated), the interplanetary magnetic field polarity (Stanford magnetic field), are given in the catalogue.

The long-term variation in the occurrence rate of high-speed streams shows interesting differences between even and odd solar cycles when catalogues for solar cycles 20, 21, and 22 are considered together. Hence, this catalogue, extended now over three solar cycles, should be useful for studies connected with solar-interplanetary or solar-terrestrial phenomena, and to clarify solar activity in time.

1. Introduction

It is known, one of the most dynamical interplanetary phenomena of solar terrestrial physics is definitely the passage of solar wind streams near the Earth environment. Previous studies of various aspects of the solar wind velocity variability with time in the ecliptic plane revealed a solar wind tendency to be organized as stream structures (e.g., Burlaga, 1974, 1979; Intrilligator, 1977; Iucci *et al.*, 1979; Toptygin, 1985, among others). In particular, the characteristics and the long-term variations in the occurrence rate of high-speed streams for solar cycles 20 and 21 have been studied by Lindblad and Lundstedt (1981) and Mavromichalaki, Vassilaki, and Marmatsouri (1988). Reference catalogues of high-speed solar wind streams observed near the Earth have been produced, considering two possible solar sources: coronal holes and active regions emitting solar flares.

A new updated reference catalogue of high-speed solar wind streams up to December 1996 (solar cycle 22) is provided in this work. This catalogue, apart from the main characteristics of the solar wind streams, contains the dominant polarity of the interplanetary magnetic field (either away or toward the Sun) for the stream duration. Cases where a sector boundary crossing ($+/-$ or $-/+$) was embedded in the solar wind streams are also included. The above are very useful for the study of the solar wind stream distribution as a function of Bartels rotation days for

Solar Physics **183:** 181–200, 1998.

various categories and for a comparison with the earlier epoch studied by Lindblad (1981) and Rangarajan and Mavromichalaki (1989). Moreover, an attempt is made to investigate, in comparison between them, the main characteristics of the fast streams identified during cycles 20, 21, and 22, suggesting that an 11-yr variation is observed in the occurrence rate of the corotating streams as well as of the flare generated streams.

2. Determination of Fast Solar-Wind Streams

In studies concerning the stream occurrence, various definitions for a high-speed stream have been used. As for example Intrilligator (1977) defines a high-speed stream as one having a rapidly rising increase in solar wind speed and a peak velocity greater than or equal to 450 km s^{-1}. Venkatesan, Shukla, and Agrawal (1982) define a high-speed solar wind stream as one having a rapidly rising increase in the solar wind speed (V) over a short period ($\Delta V \geq 200$ km s^{-1} in $\leq$24 hr) reaching a maximum value of $\geq$550 km s^{-1} and remaining at high values for at least 3 days after the increase.

In a previous contribution (Mavromichalaki, Vassilaki, and Marmatsouri, 1988) as well as in the present one, we define a high-speed solar wind stream as a period in which the difference $\Delta V_{\max}$ between the maximum daily mean speed ($V_{\max}$) and the mean value between the speeds immediately preceding and following the stream (V_0) is greater or equal to 100 km s^{-1}, lasting for at least two days (Iucci *et al.*, 1979), considering this definition for a fast-stream as more adequate for the purpose of solar-terrestrial studies. The velocity profile as well as other plasma and field data for the dates of large $\Delta V_{\max}$ were studied by visual inspection of the intensity versus time plots published in the *Interplanetary Medium Data Book* (Couzens and King, 1986; King, 1989; King and Papitashvili, 1994; Mathews and Papitashvili, 1998). The difference $\Delta V_{\max}$ was computed for the solar wind streams observed during the period January 1985 to December 1996. In order to fill out several data gaps, observations of the solar wind speed spacecraft data published in the monthly issues of the *Solar Geophysical Data* (NOAA/WDC-A, Boulder) were used.

Apart from these characteristics of the streams, we have classified them into two types: the corotating streams (CS) and the flare-generated streams (FGS).

The basic physical features of the corotating high-speed streams with respect to the most important interplanetary parameters are the following:

(a) The proton density (n) rises to unusually high values near the leading edges of the streams.

(b) The interplanetary magnetic field (B) magnitude is proportional to bulk speed with a constant polarity throughout the stream except for some fluctuations lasting a few hours.

(c) The proton temperature (T) varies in a pattern similar to that of the flow speed.

On the other side, the behaviour of interplanetary parameters during flare-generated streams has a tendency to be irregular. Generally we can say that:

(a) All the interplanetary parameters show simultaneous increases, possibly denoting radially outcoming fast shocks.

(b) The bulk speed, the proton density and magnetic field magnitude show large fluctuations in the maximum speed period, while the field polarity often shows inversions.

(c) The proton temperature behaviour tends to divert from speed behaviour.

Moreover, we can suggest that the corotating streams are emitted by coronal holes and are associated with simple decreases of cosmic rays recorded at ground based stations, whereas the flare generated streams seem to be associated with strong active regions emitting solar flares and producing Forbush decreases at the Earth (Iucci *et al.*, 1979; Mavromichalaki, Vassilaki, and Marmatsouri, 1988).

A typical example of these two types of high-speed streams is given in Figure 1. It is noted that the behaviour pattern of interplanetary parameters during the corotating stream of August 1988 is clearly different from that during the flare-generated stream of October 1988. Based on the above considerations we produced an up-to-date catalogue of high-speed streams recorded near the Earth during the period 1985–1996 as a continuation of the previous one (Mavromichalaki, Vassilaki, and Marmatsouri, 1988). In this table the first three columns give the year, month, and day, respectively, of the beginning time of a high-speed stream, defined as the 3 hr interval of the smallest speed value of the given day. The fourth and fifth columns list the Bartels rotation (number and day) corresponding to the first day of the stream. In the sixth column the dominant polarity of the interplanetary magnetic field for the duration of the stream (Lindblad, 1981) is presented. The following three columns give the day, month, and hour, respectively, of the maximum speed appearance (FDMA). The tenth and eleventh columns give the mean value (V_0) between the speeds immediately preceding and following the stream and the maximum daily mean speed (V_{max}), respectively. The next one gives the duration (DUR) of the high-speed stream in days. Finally, the last column indicates the type of the high-speed plasma stream.

3. Features of the High-Speed Streams

In this work we tried to emphasise well-defined streams. A stream was listed only if the data coverage was reasonably complete. Each stream appearance is listed separately, regardless of whether or not it is member of a recurrent series. In Table I a total of 373 individual high-speed streams are reported, where a total of 287 (77%) corotating streams and a total of 86 (23%) flare generated streams are found. It is noteworthy that the number of corotating streams is much greater than the number

TABLE I

A catalogue of high-speed solar-wind streams for the years 1985–1996 giving in each column:
– the year, month and day of the beginning time of a high-speed stream;
– the Bartels rotation (number and day) of the first day of the stream;
– the interplanetary magnetic field polarity for the stream;
– the day, month and hour of the maximum speed appearance (FMDA);
– the mean value (V_0) between the speeds immediately preceding and following the stream;
– the maximum daily mean speed (V_{max});
– the duration (Dur.); and
– the type of the high-speed stream (CS or FGS)

Y M D	Bartels rotation No. D	IMF	FDMA D M Hr	V_0	V_{max}	Dur. (days)	Type
85 01 07	2069 15	−	11 01 12	425	677	10	CS
85 01 27	2070 09	+	28 01 11	370	508	04	CS
85 02 06	2070 19	+	07 02 12	500	729	04	CS
85 02 10	2070 22	+	11 02 01	550	712	03	CS
85 02 16	2071 03	−	17 02 11	350	485	05	CS
85 02 24	2071 10	+	25 02 20	340	440	02	CS
85 03 02	2071 16	+	02 03 10	550	655	03	CS
85 03 05	2071 19	+/−	07 03 24	430	671	06	CS
85 03 14	2072 01	+	15 03 17	343	500	09	CS
85 03 27	2072 14	−/+	02 04 09	304	750	10	CS
85 04 09	2073 27	+/−	10 04 18	392	599	04	CS
85 04 25	2073 16	−/+	26 04 11	520	684	02	CS
85 05 04	2073 25	−	05 05 08	360	520	05	CS
85 05 15	2074 10	+	16 05 21	315	440	04	CS
85 05 28	2074 22	−/+	29 05 03	307	468	03	CS
85 05 31	2074 25	+/−	01 06 07	317	465	05	CS
85 06 24	2075 22	+/−	27 06 05	355	621	03	CS
85 06 27	2075 25	+/−	28 06 20	460	684	04	CS
85 07 01	2076 02	−/+	07 07 10	450	707	10	FGS
85 07 17	2076 18	−/+	18 07 10	337	500	05	CS
85 07 23	2076 23	+	26 07 06	455	606	04	CS
85 07 30	2077 04	−/+	01 08 20	337	644	07	CS
85 08 12	2077 17	−	13 08 10	325	644	05	CS
85 08 18	2077 22	+	18 08 22	340	554	03	CS
85 08 25	2078 02	+	28 08 17	450	736	07	CS
85 09 08	2078 16	−	10 09 07	315	503	06	CS
85 09 19	2079 01	+/−	21 09 08	500	694	04	CS
85 09 23	2079 05	−/+	25 09 11	500	629	04	CS
85 10 05	2079 16	−	06 10 13	325	705	06	CS

TABLE I
Continued

Y M D	Bartels rotation No. D	IMF	FDMA D M Hr	V_0	V_{max}	Dur. (days)	Type
85 10 17	2080 02	−	19 10 10	467	716	04	CS
85 11 02	2080 18	−	03 11 13	385	619		CS
85 11 09	2080 25	+	09 11 17	500	670	02	CS
85 11 12	2081 01	+/−	15 11 15	440	701		CS
85 11 26	2081 15	+/−	27 11 23	300	493	03	CS
85 12 03	2081 22	−	05 12 02	553		02	CS
85 12 09	2082 01	+/−	10 12 24	355	716		CS
85 12 18	2082 10	−/+	19 12 20	458		04	CS
85 12 30	2082 22	−	02 01 08	600	748	05	CS
86 01 25	2083 16	−/+	28 01 10	450	794	07	CS
86 02 06	2084 05	+	09 02 07	350	926	08	CS
86 02 20	2084 19	+	23 02 20	450	790	08	CS
86 03 06	2085 06	−	09 03 04	375	696	04	CS
86 03 17	2085 17	+	19 03 03	380	532	02	CS
86 03 21	2085 21	−/+	23 03 03	385	647	05	CS
86 03 26	2085 27		27 03 15	387	679	04	CS
86 03 31	2086 05	+	04 04 01	400	539		CS
86 04 22	2086 27	+	24 04 10	400	615	05	CS
86 04 27	2087 05	+	29 04 15	350	513		CS
86 05 30	2088 10	−	01 06 05	360	533	06	CS
86 06 27	2089 12	−/+	01 07 01	337	572	06	FGS
86 07 24	2090 11	+/−	26 07 04	380	728	08	FGS
86 08 03	2090 22	+/−	04 08 15	420	627	05	CS
86 08 12	2091 04	+	13 08 13	338	514	05	CS
86 08 20	2091 11			325			CS
86 08 28	2091 20	+/−	30 08 02	565	781	05	CS
86 09 11	2092 06	−/+	12 09 22	375	596	04	FGS
86 09 15	2092 10		20 09 10	425	697	08	CS
86 09 23	2092 18	+/−	25 09 13	435	743	08	CS
86 10 05	2093 03	−/+	06 10 11	400	565	04	CS
86 10 13	2093 08	+	15 10 04	440	683	04	CS
86 10 18	2093 16	+	19 10 10	400	684	09	CS
86 10 28	2093 27	+/−	29 10 07	350	498	04	CS
86 11 01	2094 05						CS
86 11 10	2094 13	+	12 11 06	365	504	03	CS
86 11 15	2094 18		16 11 02	350	541	07	CS
86 11 23	2094 26	+/−	24 11 05	355	519	05	FGS

TABLE I
Continued

Y M D	Bartels rotation No. D	IMF	FDMA D M Hr	V_0	V_{max}	Dur. (days)	Type
86 12 21	2095 27	+/−	23 12 16	375	583	09	CS
86 12 31	2096 09		02 01 18	330	432	05	CS
87 01 28	2097 11	−/+	29 01 01	380	521	03	CS
87 02 06	2097 19	−/+	08 02 23	360	572	05	CS
87 02 20	2098 06	−/+	20 02 15	365	652	07	CS
87 03 04	2098 18	−/+	07 03 15	410	612	07	CS
87 03 18	2099 06	+	19 03 08	410	568	03	CS
87 03 21	2099 08	−/+	22 03 24	350	684	11	CS
87 04 04	2099 23	+	04 04 05	300	409		FGS
87 04 10	2100 02	+/−	10 04 10	330	457	03	CS
87 05 09	2101 03	+	09 05 15	335	443	04	CS
87 05 22	2101 17	−	24 05 23	300	432	08	CS
87 06 01	2101 27	+	02 06 16	350	494	04	CS
87 06 11	2102 09	+/−	13 06 05	350	518	04	CS
87 06 25	2102 23	+/−	26 06 13	315	489	03	CS
87 07 07	2103 09	−/+	08 07 13	345	457	05	CS
87 07 16	2103 16	+	20 07 11	340	511	08	CS
87 08 04	2104 10	+/−	05 08 03	355	486	04	CS
87 08 09	2104 14	+/−	14 08 18	355	692	11	CS
87 08 26	2105 04	−/+	26 08 14	400	560	04	CS
87 08 31	2105 09	−	01 09 16	400	675	05	CS
87 09 07	2105 16	+/−	08 09 05	385	618	03	CS
87 09 10	2105 19	+/−	14 09 02	350	730		CS
87 09 25	2106 07	−/+	26 09 01	355	475	02	FGS
87 10 07	2106 20	−/+	07 10 24	335	459	03	CS
87 10 13	2106 26	+	15 10 14	350	783	09	CS
87 10 23	2107 06	−	28 10 08	345	704	10	CS
87 11 02	2107 18	−/+	03 11 21	360	504	06	FGS
87 11 09	2107 20	+	13 11 10	385	695	08	CS
87 11 11	2108 01	+	13 11 10	425	695	06	CS
87 11 23	2108 12	−	24 11 24	380	608	04	FGS
87 12 05	2108 24	+	06 12 08	370	618	04	CS
87 12 10	2109 02	+/−	10 12 24	325	692	11	FGS
87 12 21	2109 14	−	22 12 17	350	450	02	CS
88 01 01	2109 25	−/+	02 01 20	300	477	03	CS
88 01 13	2110 09	+/−	14 01 08	340	732	06	FGS
88 02 06	2111 07	−/+	06 02 14	330	472	03	CS

TABLE I
Continued

Y M D	Bartels rotation No. D	IMF	FDMA D M Hr	V_0	V_{max}	Dur. (days)	Type
88 02 12	2111 13		13 02 01	400	509		CS
88 02 22	2111 23	−	22 02 17	370	491	04	CS
88 03 03	2112 06	−/+	04 03 17	335	473	04	CS
88 03 07	2112 10	+	15 03 01	325	631	13	CS
88 04 09	2113 16	+	10 04 13	420	618	03	CS
88 04 22	2114 02	−	23 04 20	330	529	04	CS
88 05 06	2114 16	+/−	06 05 09	350	666	07	CS
88 05 16	2115 03	+	22 05 01	325	503	07	CS
88 05 29	2115 12	+	31 05 08	325	454	06	FGS
88 06 14	2116 01	+/−	15 06 19	365	439	03	CS
88 06 29	2116 16		01 07 04	325	640	08	FGS
88 07 20	2117 10	−	21 07 08	425	594	03	FGS
88 08 13	2118 08	−	15 08 11	450	658	03	CS
88 08 20	2118 14		25 08 20	390	700	10	CS
88 08 31	2118 25	−	01 09 13	375	596	03	FGS
88 09 10	2119 08	+/−	11 09 16	300	538	05	FGS
88 09 19	2119 17	+	20 09 11	597		07	FGS
88 09 26	2119 27	+	26 09 24	407	513	03	CS
88 10 04	2120 05	+/−	06 10 02	290	563	04	FGS
88 10 15	2120 16		19 10 08	300	729	09	CS
88 10 26	2121 02	−	28 10 21	397	492	05	CS
88 10 30	2121 04	+	31 10 14	300	433	02	CS
88 11 02	2121 07	+	03 11 04	340	532	06	CS
88 11 12	2121 17	−	15 11 18	370	610	09	CS
88 11 25	2122 03	+	27 11 16	350	494	03	CS
88 12 03	2122 11	−	04 12 02	524		07	CS
88 12 17	2122 25	+	18 12 05	500	833	07	CS
88 12 28	2123 09	+	29 12 21	400	727	07	CS
89 01 10	2123 23	−/+	11 01 21	744		05	FGS
89 01 14	2123 25	+	15 01 21	425	713	04	CS
89 01 23	2124 08	−	24 01 02	678		07	CS
89 02 04	2124 20	−	05 02 10	694		08	CS
89 02 19	2125 08	+	20 02 15	420	577	04	CS
89 03 01	2125 19	−	03 03 10	435	618	02	CS
89 03 04	2125 21	−	06 03 11	440	664	05	CS
89 03 08	2125 25	−/+	08 03 19	400	551		FGS
89 03 14	2126 04	+	19 03 12	880		04	FGS

TABLE I
Continued

Y M D	Bartels rotation No. D	IMF	FDMA D M Hr	V_0	V_{max}	Dur. (days)	Type
89 03 27	2126 17	−	01 04 11	420	765	08	CS
89 04 08	2127 02	+/−	09 04 06	330	503	04	CS
89 04 24	2127 17		29 04 06	360	686	07	FGS
89 05 04	2128 01		05 05 08	410	612	03	CS
89 05 07	2128 04		08 05 01	364	514	05	CS
89 05 23	2128 18		24 05 03	400	712		FGS
89 06 13	2129 14	−	13 06 22	375	550	03	FGS
89 07 06	2130 10	−/+	07 07 08	380	510	04	CS
89 08 14	2131 21	−	15 08 07	405	672	03	FGS
89 08 17	2131 25	−/+	18 08 15	485	671	02	FGS
89 08 26	2132 07	+	27 08 23	330	517	08	FGS
89 09 08	2132 20	−/+	08 09 08	495			CS
89 09 20	2133 05	−	22 09 13	340	508	03	CS
89 10 08	2133 23	+	10 10 02	390	622	05	CS
89 10 18	2134 06	−	21 10 02	345	916		FGS
89 10 29	2134 17	+	30 10 12	430	635	03	CS
89 11 08	2134 27	+	09 11 08	330	675	08	FGS
89 11 21	2135 13	−/+	21 11 14	525			CS
89 11 27	2135 18	+	28 11 23	350	739		FGS
89 12 07	2136 02	+	08 12 12	400	532	03	CS
89 12 16	2136 11	+	17 12 13	365	498	03	CS
89 12 21	2136 16		23 12 19	390	516	05	FGS
89 12 29	2136 24	+/−	29 12 21	500	740	03	FGS
90 01 03	2137 02	+/−	05 01 19	450	639	03	FGS
90 01 23	2137 21	−	24 01 07	520	748	05	CS
90 01 29	2138 01	−	29 01 22	370	507		CS
90 02 04	2138 07	−/+	05 02 09	380	665	06	CS
90 02 22	2138 25	−	23 02 18	410	611	03	CS
90 03 01	2139 05	−/+	02 03 06	546		04	CS
90 03 05	2139 09	+/−	06 03 09	380	493	03	CS
90 03 18	2139 22	−	18 03 21	315	501	02	FGS
90 03 20	2139 24	−	21 03 12	365	623	04	CS
90 03 30	2140 06	+	30 03 24	370	616	04	CS
90 04 12	2140 19	−	12 04 14	350	757	05	FGS
90 04 22	2141 03	−	24 04 14	365	521	05	CS
90 05 04	2141 15	+	05 05 13	525		03	CS
90 05 10	2141 21		10 05 12	345	526		FGS
90 05 19	2142 03	−	21 05 23	400	551	04	CS

TABLE I
Continued

Y M D	Bartels rotation No. D	IMF	FDMA D M Hr	V_0	V_{max}	Dur. (days)	Type
90 05 29	2142 13	+/−	30 05 22	340	594	05	CS
90 06 12	2142 27	+	17 06 06	350	732	05	FGS
90 07 19	2144 10	+/−	20 07 24	400	552	05	CS
90 08 01	2144 22	+/−	01 08 18	335	609	05	CS
90 08 06	2145 01		07 08 03	350	481		CS
90 08 14	2145 09	−/+	16 08 16	400	699	06	CS
90 08 26	2145 20	+/−	26 08 09	460	785	04	CS
90 08 30	2145 25	−/+	31 08 02	400	572	02	CS
90 09 11	2146 10	−	12 09 02	390	551	03	CS
90 09 20	2146 19	−	21 09 15	378	482	05	FGS
90 10 02	2147 04	+	04 10 19	330	542	07	CS
90 10 09	2147 11		10 10 08	360	493	04	CS
90 10 19	2147 21	−/+	20 10 22	345	482	03	CS
90 10 29	2148 04	−/+	31 10 18	385	603	06	CS
90 11 11	2148 17	+	12 11 07	375	497	03	FGS
90 11 27	2149 05	+/−	28 11 27	330	579	03	CS
90 12 04	2149 13	−	05 12 11	350	499	04	CS
91 01 25	2151 11	+/−	26 01 14	390	559	04	CS
91 02 10	2151 27	−	11 02 23	350	459	02	CS
91 02 20	2151 10	+	23 02 16	300	546	06	CS
91 03 14	2152 21	−	09 03 24	330	568	06	FGS
91 04 02	2153 06	−/+	03 04 12	340	666	05	FGS
91 04 11	2154 06	+	12 04 21	310	426	04	CS
91 04 24	2154 19	−/+	24 04 24	375	521	03	FGS
91 05 21	2155 19	+/−	23 05 15	335	538	06	FGS
91 05 31	2156 02	−/+	01 06 06	465	665	04	FGS
91 06 04	2156 06		05 06 01	415	710	02	FGS
91 06 25	2156 27	+/−	25 06 24	530	678	05	CS
91 07 08	2157 13	−	09 07 06	400	731	03	CS
91 07 22	2157 27		23 07 03	495	625	05	FGS
91 08 01	2158 10	−/+	03 08 21	330	731	07	CS
91 08 14	2158 22		16 08 04	480	843	04	CS
91 08 18	2158 27	+	18 08 23	520	748	03	FGS
91 08 27	2159 09	−	27 08 24	345	468	03	CS
91 08 30	2159 12	−	01 09 22	365	661	06	CS
91 09 08	2159 20	−/+	13 09 24	340	582	08	CS
91 09 25	2160 11	−	27 09 10	330	547	06	FGS
91 10 06	2160 21	+/−	07 10 14	430	757	05	CS

TABLE I
Continued

Y M D	Bartels rotation No. D	IMF	FDMA D M Hr	V_0	V_{max}	Dur. (days)	Type
91 10 27	2161 16	+/−	28 10 16	525	994	04	FGS
91 10 31	2161 20	+/−	31 10 24	525	936	03	FGS
91 11 03	2161 23		03 11 12	500	757		CS
91 11 14	2162 07	+	15 11 13	340	540	02	FGS
91 11 21	2162 14	−/+	22 11 08	420	771	07	CS
91 12 02	2161 25	−/+	04 12 24	350	587	05	CS
91 12 09	2163 04	−/+	11 12 24	340	556	06	CS
91 12 16	2163 12		17 12 19	385	633	04	CS
91 12 20	2163 16	+	21 12 13	343	700	05	CS
92 01 14	2164 14	+/−	16 01 24	365	744	07	CS
92 02 08	2165 12		08 02 16	350	595	05	FGS
92 02 21	2165 25		20 02 23	355	507	03	CS
92 03 08	2166 14	+	09 03 01	345		05	CS
92 03 17	2166 22	+	17 03 20	365	576	03	FGS
92 04 03	2167 12		07 04 14	340	635	08	CS
92 05 09	2168 21		09 05 24	320	887	04	FGS
92 05 19	2169 05	−	20 05 14	300	420	03	CS
92 05 22	2169 08		22 05 06	305	456		FGS
92 05 29	2169 15	−/+	30 05 05	420	768	06	CS
92 06 10	2169 27		12 06 17	310	493	06	FGS
92 06 24	2170 13	−/+	25 06 01	430	687	04	CS
92 07 22	2171 14	−/+	23 07 02	340	681	03	FGS
92 07 30	2171 23	+	01 08 05	345	498	05	FGS
92 08 15	2172 12	+/−	16 08 14	335	476	04	CS
92 09 09	2173 10	−	09 09 05	385	589	05	FGS
92 09 17	2173 18	+	19 09 14	400	609	06	CS
92 10 13	2174 17	+/−	15 10 01	400	775	06	CS
92 10 26	2175 03	−	27 10 10	400	568	02	FGS
92 11 02	2175 08			400		03	FGS
92 11 09	2175 16	+	11 11 23	440	687	07	CS
92 11 22	2176 03	−/+	23 11 09	315	469	06	CS
92 12 07	2176 17	+/−	09 12 18	345	754	04	CS
93 01 01	2177 16	−/+	04 01 20	420	792	08	CS
93 01 13	2178 01	−/+	15 01 24	400	603	05	CS
93 01 24	2178 12	−/+	25 01 24	335	629	06	CS
93 02 06	2178 25	−	08 02 24	415	706	04	CS
93 02 20	2179 12	+	21 02 24	397	764	05	CS
93 02 28	2179 19		03 03 09	355	568	06	FGS

TABLE I
Continued

Y M D	Bartels rotation No. D	IMF	FDMA D M Hr	V_0	V_{max}	Dur. (days)	Type
93 03 08	2180 01		09 03 08	370	680	04	CS
93 03 21	2180 14	+	21 03 17	420	721	03	CS
93 04 08	2181 05		10 04 09	440	574	04	CS
93 04 12	2181 09	+/−	13 04 19	380	593	04	CS
93 04 19	2181 16	+	21 04 14	435	701	06	CS
93 05 06	2182 06	−/+	09 05 21	335	749	07	CS
93 05 18	2182 18	+	20 05 07	370	558	04	CS
93 05 28	2183 01	+/−	29 05 05	330	615	06	CS
93 06 03	2183 07		04 06 15	320	776	05	CS
93 06 10	2183 14	+	12 06 20	370	549	07	CS
93 06 23	2183 27		24 06 16	320	763	07	CS
93 07 07	2184 14	+	11 07 19	360	615	06	CS
93 07 20	2184 27	−/+	20 07 22	335	559	05	CS
93 08 04	2185 15	−	05 08 22	300	457	05	CS
93 08 15	2185 26		16 08 24	345	764	05	CS
93 08 27	2186 11	−/+	05 09 21	340	555	05	CS
93 09 04	2186 19	−	06 09 01	300	551	07	CS
93 09 22	2187 10		25 09 22	325	509	13	CS
93 10 12	2188 03	−	13 10 22	310	478	04	CS
93 10 26	2188 17	−	27 10 19	400	631	05	CS
93 11 06	2189 01	+/−	08 11 08	400	613	07	CS
93 11 25	2189 20	+	26 11 22	400	513	03	CS
93 12 01	2189 26	−/+	02 12 20	510	773	07	CS
93 12 15	2190 13	+/−	17 12 23	440	710	06	CS
94 01 01	2191 02	+	02 01 12	330	609	04	CS
94 01 11	2191 12	−	12 01 20	320	756	04	CS
94 01 25	2191 26	+	28 01 11	300	603	06	CS
94 02 05	2192 09	−	09 02 14	400	805	08	CS
94 02 19	2192 23		20 02 10	475	577	02	CS
94 02 21	2192 25	+	21 02 20	445	919	06	FGS
94 02 29	2193 05	−	02 03 22	390	513	05	CS
94 03 06	2193 10	−	08 03 05	380	748	05	CS
94 03 13	2193 17	+	15 03 24	490	769	08	CS
94 04 03	2194 11	−	08 04 05	395	839	19	CS
94 05 01	2195 12	−	09 05 03	500	824	09	CS
94 05 14	2195 25	+	16 05 11	405	817	08	CS
94 05 28	2196 12	−	31 05 09	440	786	12	FGS
94 06 10	2196 25	+	13 06 12	395	728	09	CS

TABLE I
Continued

Y M D	Bartels rotation No. D	IMF	FDMA D M Hr	V_0	V_{max}	Dur. (days)	Type
94 06 19	2197 07	−	21 06 04	365	674	05	CS
94 06 26	2197 14	−	03 07 09	365	670	11	CS
94 07 06	2197 26	+	08 07 03	350	455	05	FGS
94 07 14	2198 07	−	16 07 24	380	817	07	CS
94 07 21	2198 14	−	21 07 20	370	540	03	FGS
94 07 27	2198 20	+	30 07 01	360	648	07	CS
94 08 10	2199 07	−	14 08 07	280	662	10	CS
94 08 27	2199 23	−	27 08 11	340	541	03	CS
94 09 04	2200 04	−	09 09 19	300	711	08	CS
94 09 16	2200 16	+	18 09 02	320	539	06	CS
94 10 03	2201 06	−	04 10 15	340	720	05	CS
94 10 12	2201 15	+	15 10 12	345	583	06	CS
94 10 21	2201 26	+	24 10 07	300	633	06	CS
94 11 09	2202 18	−/+	10 11 14	365	579	05	CS
94 11 18	2202 27	−/+	20 11 11	360	493	03	FGS
94 12 01	2203 13	−	02 12 22	320	588	04	CS
94 12 06	2203 18	−/+	07 12 16	330	701	08	CS
94 12 15	2203 27	+	16 12 13	370	636	06	CS
94 12 20	2204 04	+/−	20 12 16	340	610	13	CS
95 01 01	2204 17		08 01 14	360	566	10	CS
95 01 22	2205 11	−	23 01 13	310	438	05	FGS
95 01 27	2205 17	−/+	02 02 14	345	657	10	CS
95 02 08	2206 01	−	14 02 14	350	639	14	CS
95 02 26	2206 19	+/−	01 03 14	355	673	09	CS
95 03 09	2207 03		14 03 09	350	774	08	CS
95 03 26	2207 19	+	29 03 06	335	544	07	FGS
95 04 06	2208 03	+	08 04 05	300	683	12	FGS
95 04 21	2208 18	+	25 04 02	250	499	09	CS
95 05 02	2209 02	+	03 05 02	340	744	13	CS
95 05 16	2209 16	+	16 05 19	350	500	06	CS
95 05 23	2209 23	−	24 05 06	430	663	03	CS
95 05 29	2210 02	+	31 05 14	340	768	12	CS
95 06 09	2210 13	−	09 06 23	305	398	04	CS
95 06 19	2210 23	−	19 06 22	355	676	08	FGS
95 06 25	2211 03	+	25 06 22	360	562	08	CS
95 07 14	2211 21	−	17 07 17	390	687	07	CS
95 08 07	2212 18	+	10 08 05	360	600	07	CS
95 09 05	2213 20	+	07 09 16	310	611	07	FGS

TABLE I
Continued

Y M D	Bartels rotation No. D	IMF	FDMA D M Hr	V_0	V_{max}	Dur. (days)	Type
95 09 13	2214 02	+	09 16 10	330	526	07	CS
95 09 26	2214 15	+	09 28 01	300	415	05	FGS
95 10 09	2215 01	+	12 10 07	310	534	09	CS
95 10 20	2215 12	−	24 10 09	320	446	06	CS
95 11 04	2215 27	+	06 11 06	365	592	08	CS
95 11 27	2216 21	−	29 11 08	350	506	04	FGS
95 12 15	2217 14	−	18 12 01	310	418	04	FGS
95 12 23	2217 23	−	26 12 11	370	596	05	CS
95 12 30	2218 02	−		310		13	CS
96 01 12	2218 15	−	18 01 13	320	506	11	CS
96 01 25	2219 01	−	31 01 16	385	549	07	CS
96 02 02	2219 09	−	04 02 19	365	404	05	CS
96 02 07	2219 14	+	12 02 14	335	582	11	CS
96 02 16	2219 23	+/−	19 02 10	360	517	07	CS
96 02 22	2220 02	−	26 02 21	300	581	09	CS
96 03 08	2220 17	−	13 03 09	350	572	10	CS
96 03 19	2221 01	−	21 03 23	400	655	05	CS
96 03 24	2221 06	−	25 03 15	400	594	05	CS
96 04 08	2221 21	+	09 04 12	286	491		CS
96 04 17	2222 03	−	20 04 08	420	727	06	CS
96 05 13	2223 01	−	15 05 14	335	511	06	CS
96 05 29	2223 18	+	30 05 01	310	463	08	CS
96 06 05	2223 25	+	06 06 13	315	471	02	CS
96 06 19	2224 12	−	19 06 09	365	554	05	FGS
96 07 03	2225 04	−	04 07 01	340	532	05	CS
96 07 11	2225 12	−	13 07 09	310	416	06	FGS
96 07 17	2225 18			335		08	CS
96 07 30	2226 04	−	31 07 15	332	525	07	CS
96 08 12	2226 17	−/+	18 08 11	335	491	08	CS
96 08 25	2227 03	−	30 08 21	330	518	10	CS
96 09 04	2227 13	+	12 09 23	375	689	13	CS
96 09 24	2228 06	−	27 09 01	360	626	09	FGS
96 10 08	2228 20	+	10 10 03	355	516	04	CS
96 10 12	2228 24	+	14 10 11	385	535	06	CS
96 10 21	2229 06	−	23 10 10	370	638	06	CS
96 10 27	2229 12			335		08	CS
96 11 03	2229 19	−/+	04 11 04	325	441	06	FGS
96 11 09	2229 25	+	15 11 02	320	497	08	CS

TABLE I
Continued

Y M D	Bartels rotation No. D	IMF	FDMA D M Hr	V_0	V_{max}	Dur. (days)	Type
96 11 22	2230 11	$-$	28 11 04	330	492	10	CS
96 12 02	2230 21	$+$	04 12 12	280	500	07	CS
96 12 09	2231 01	$-$	11 12 10	370	668	06	CS
96 12 14	2231 06	$-$	16 12 01	420	568	04	CS
96 12 21	2231 13	$+/-$	23 12 16	290	421	06	CS

of flare-generated streams during the current solar cycle. The yearly distribution of the two types of streams and the total number occurring during the period 1985 –1996 is reported on the right side of Figure 2. The small number of observed flare-generated high-speed streams during this solar cycle is also noteworthy. We add that the observed two peaks in 1989 and 1991 are consistent with the cosmic-ray flux minima expected during the maximum phase at each sunspot cycle (e.g., Storini and Felici, 1994; Marmatsouri *et al.*, 1995; Storini, 1995; Storini and Pase, 1995; Storini *et al.*, 1997, and references therein).

For completeness, the yearly distribution of the two types of streams as well as the total number of them during solar cycles 20 and 21 are also shown in Figure 2. The occurrence of the fast streams during cycle 20 has been taken from Lindblad and Lündstedt (1981) and for cycle 21 from Mavromichalaki, Vassilaki, and Marmatsouri (1988). A large number of flare-generated streams appearing during solar maxima occurred at the years 1969, 1979, 1989 of cycles 20, 21, 22, respectively, as was expected. On the other hand, the existence of large coronal holes during solar minimum most likely gives a lot of corotating streams. Storini (1995) underlined that there are essential differences in the behaviour of the Sun during the declining phases of different solar cycles, such as high-speed solar wind streams coming from coronal holes during the declining phases of cycles 20 and 21 which affected the cosmic-ray propagation.

It is also concluded from Figure 2 that the activity of the 21st solar cycle, which is an odd cycle, was greater than the activity of the 20th and 22nd solar cycles. So a clear 11-yr variation in the occurrence rate of the fast streams is apparent following the solar cyclic variation. Different behaviour of them between even and odd solar cycles is probably due to the 22-yr variation of the solar magnetic field (Legrand and Simon, 1981; Simon and Legrand, 1992; Mavromichalaki *et al.*, 1997). This is consistent with the fact that the odd cycles are more active than the even cycles which is reported by many authors. For example Swinson, Koyama, and Saito (1986) showed that northern solar hemisphere activity was displayed as north-south asymmetry peaks about two years after sunspot minimum, which is

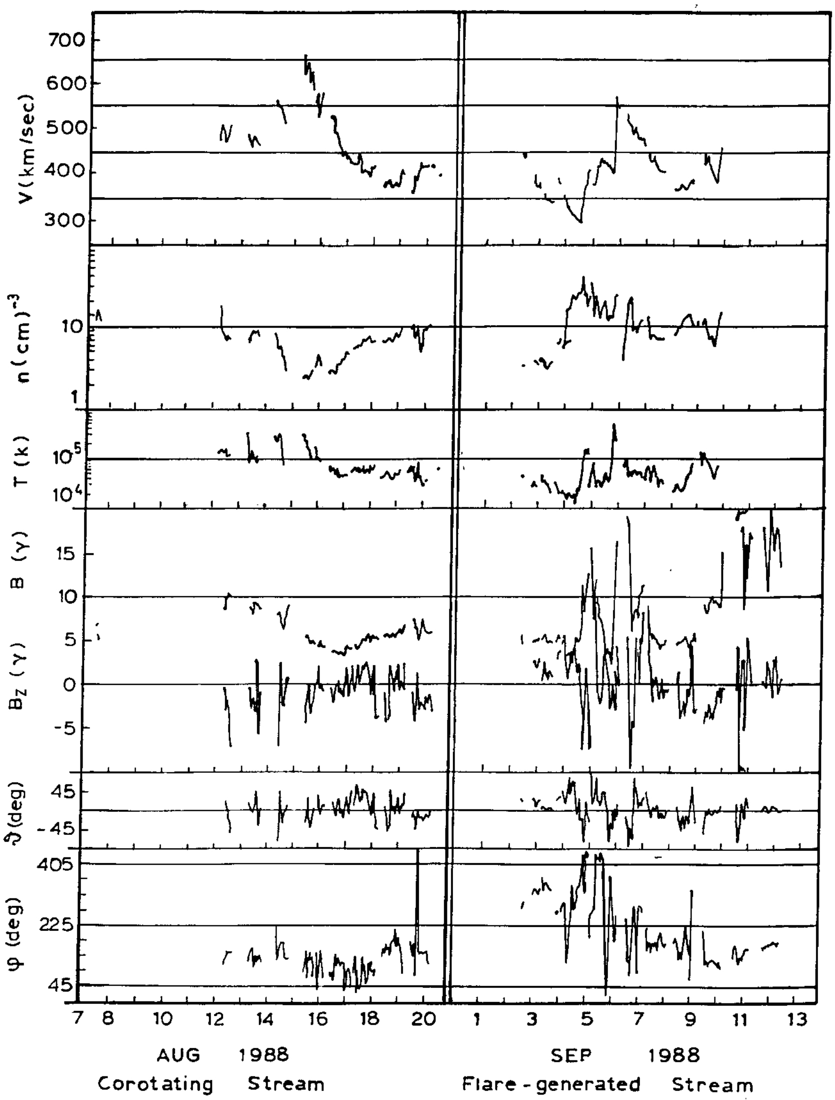

Figure 1. A typical example of the two types of high-speed solar wind streams identified in this catalogue.

greater during even cycles. This asymmetry is related to the 22-yr solar magnetic cycle. Storini and Sýkora (1997) recently verified the validity of the Gnevyshev –Ohl rule in green corona brightness. According to this rule, if sunspot number (R_z) cycles are organized in pairs of even-odd numbered cycles, the height of the peak in the curve of the yearly averaged sunspot numbers R_z is always lower for a given even cycle in comparison with the corresponding height of the following odd cycle. Mavromichalaki, Belehaki, and Rafios (1998) noted many differences between even and odd solar cycles in cosmic-ray intensity at neutron monitor en-

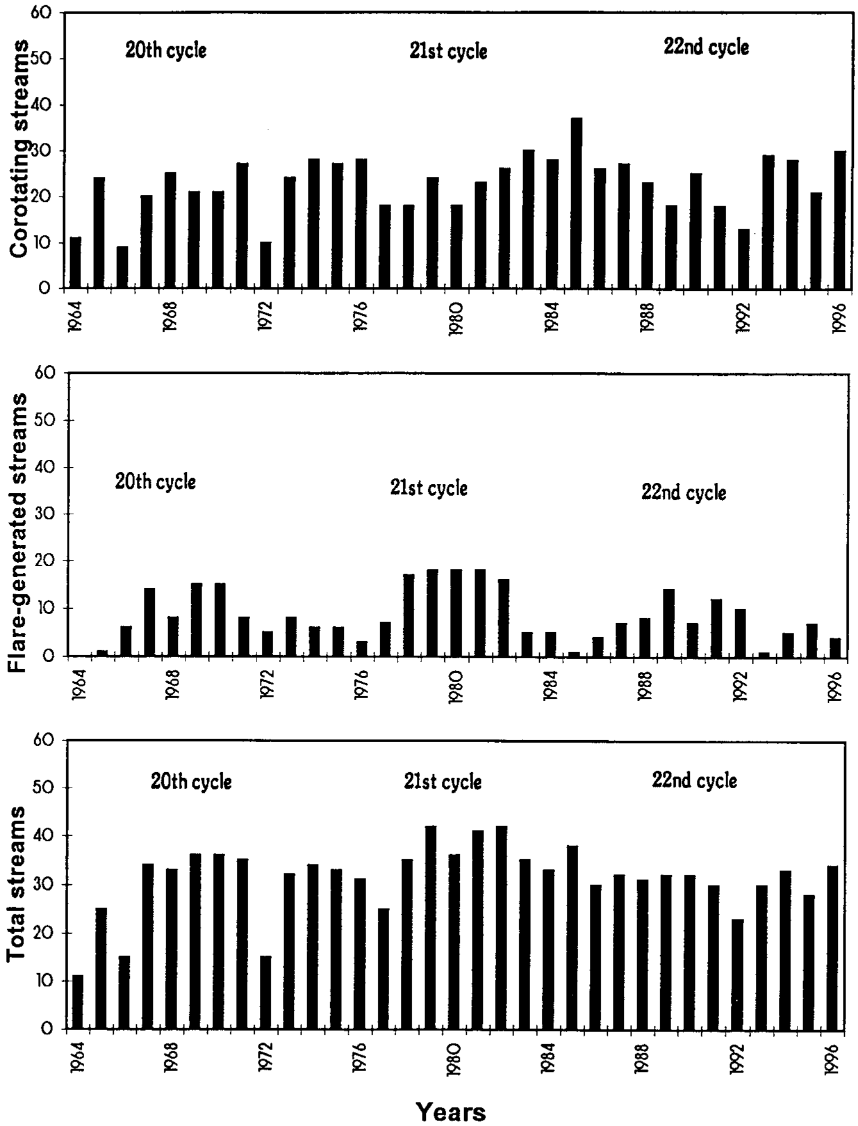

Figure 2. Histograms showing the distribution of the total number of fast streams (*bottom panel*), the number of corotating streams (*top panel*) and the flare-generated streams (*middle panel*) for the solar cycle 22 together with the solar cycles 20 and 21.

ergies related to the 22-yr magnetic cycle and to polarity reversals of the polar magnetic field of the Sun.

In Figure 3 histograms show the duration of the total number of fast streams during the three cycles. It is noteworthy that the distribution of the stream durations shows a maximum around 4–6 days for the even cycles and about 6–8 days for the odd cycle. It is also in agreement with the fact that the 21st cycle is characterised by

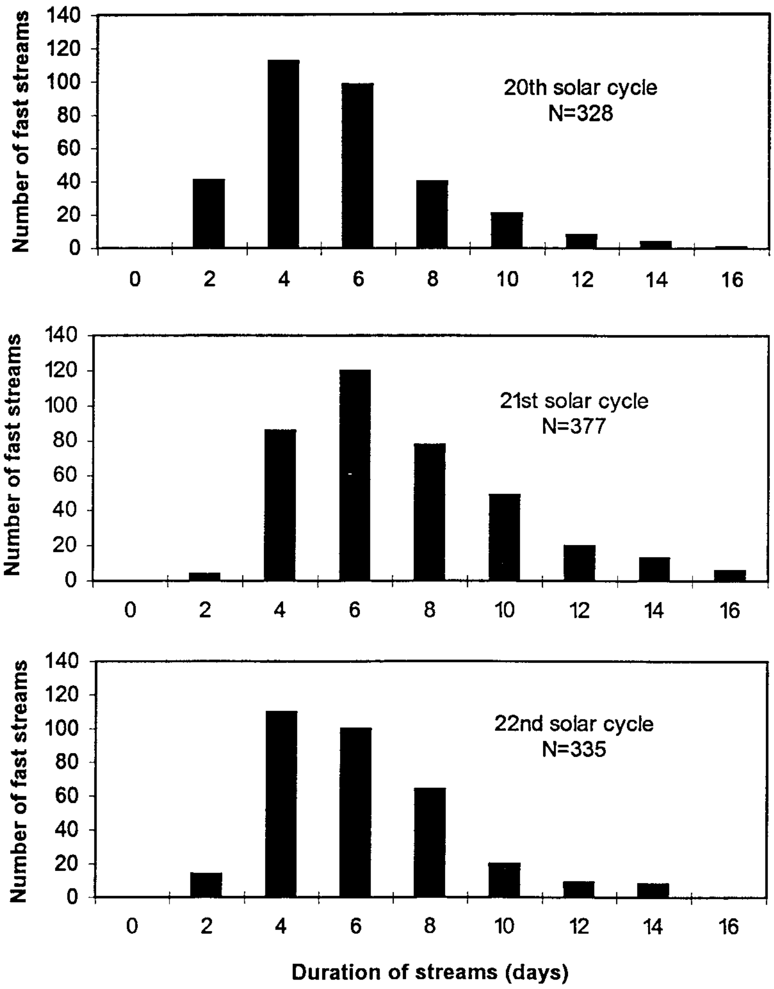

Figure 3. The time duration of high-speed solar wind streams for cycles 20, 21, and 22.

higher activity than the other ones. Mavromichalaki, Belehaki, and Rafios (1998) showed that during the 21st solar cycle the solar flares affected mainly the cosmic-ray modulation and not the sunspot number, as in the 20th solar cycle. The sunspot parameter is not always the right index for solar-induced effects in the interplanetary medium. It seems to be a natural consequence of the Gnevyshev–Ohl rule where each 22-yr solar activity cycle begins with an even numbered sunspot cycle (lower than the following odd cycle) and ends with an odd numbered one (higher than the preceding even cycle) (Gnevyshev and Ohl, 1987).

A seasonal variation is also observed in the occurrence rate of the two types of streams and the total number of them. Two maxima appeared during March and August (Figure 4). This phenomenon may be related to the asymmetric variation

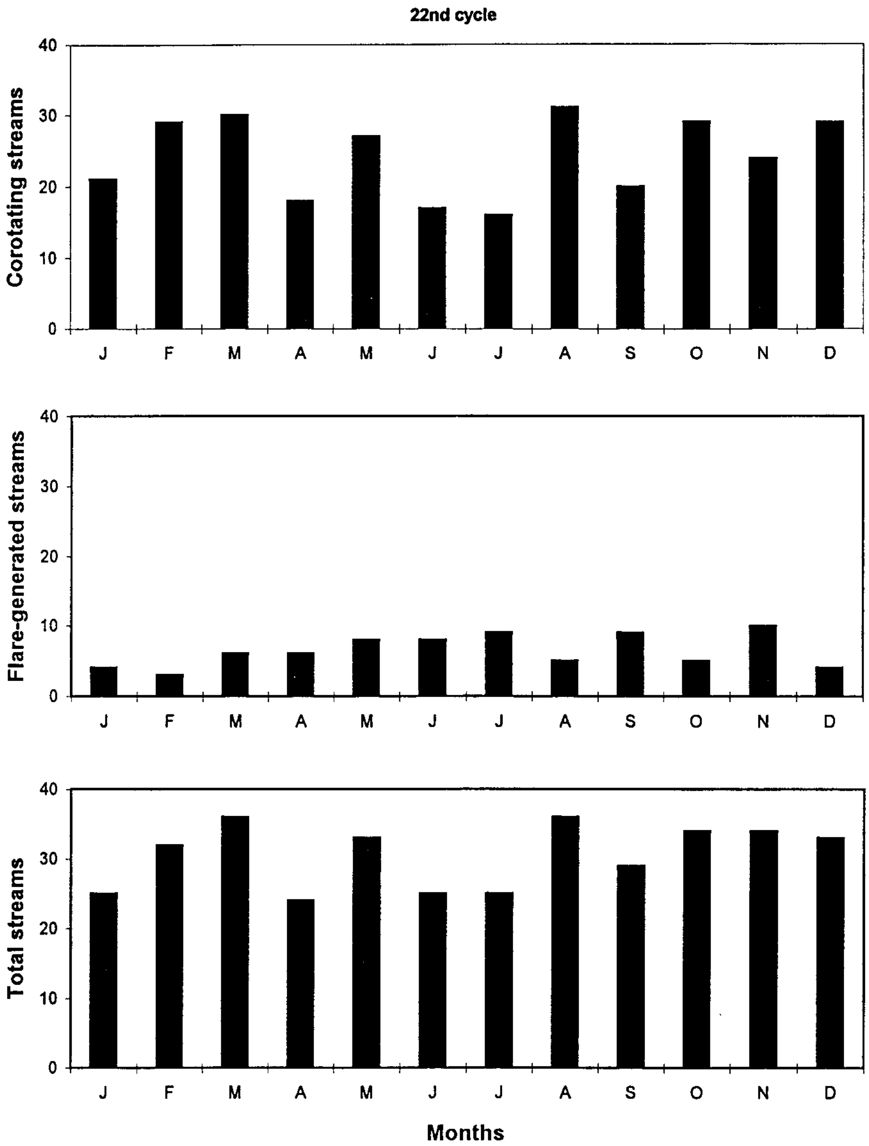

Figure 4. Superposed epoch analysis of the number of fast solar wind streams during the period 1985 –1996.

of the emissions of the solar corona (Xanthakis *et al.*, 1994). This variation may be attributed to the motion of the Sun towards the apex, which causes activity enhancements in the solar hemisphere which faces this point. An epoch analysis of the east-west differences of the green coronal absolute brightness of the Pic-du-Midi Observatory reveals a maximum east-west inequality of this intensity when the Earth stands on the equinoxes (September and March).

4. Conclusions

From all of above, the following conclusions can be drawn.

A new catalogue of the fast streams recorded near the Earth is obtained, as a continuation of previous ones. It is believed that this catalogue, extended now over three solar cycles, may be found very useful for studies of various solar-interplanetary and solar-terrestrial phenomena. A solar cycle variation is present in the occurrence rate of the corotating as well as of the flare-generated streams. The large number of flare-generated streams during the odd cycle (21st), the appearance of two maxima of them during the even cycles (20th, 22nd) are some characteristics which indicate different behaviour between even and odd solar cycles. Another characteristic is that the duration of the fast streams is greater in the odd cycle which appeared more active than that of the even cycles.

A seasonal variation of the streams is also observed with two maxima during March and July–August. It is noted that the same modulation also appeared in the coronal emission line intensities and K-corona measurements (Xanthakis *et al.*, 1994).

Conclusively, we can say that the observed differences in the distribution patterns between solar cycles may be attributed to the intrinsic differences in solar activity and interplanetary magnetic field between the cycles.

In the future, the study of the distribution of the occurrence of the streams as a function of Bartels rotation days using the dominant polarity of the IMF associated with the referred fast streams will be very useful to determine the sector structure of the interplanetary magnetic field.

Acknowledgements

The authors are indebted to the National Space Flight Center for placing at our disposal the interplanetary medium data compiled by J. King and co-authors. Thanks are also due to Mrs P. Tatsi for technical help.

References

Burlaga, L. R.: 1974, *J. Geophys. Res.* **79**, 3717.
Burlaga, L. R.: 1979, *Space Sci. Rev.* **17**, 327
Couzens, D. A. and King, J: 1986, *Interplanetary Medium Data Book NSSCD/WDC-A -R@S89-04*, Goddard Space Flight Center, Greenbelt, Maryland.
Gnevyshev M. N. and Ohl, A. I.: 1987, *Soln. Dannye* No. 8, 90.
Intrilligator, D.: 1977, in M. Shea *et al.* (eds.), *Study of Travelling Interplanetary Phenomena*, D. Reidel Publ Co., Dordrecht, Holland, p. 195.
Iucci, N., Parisi, M., Storini, M., and Villoresi, G.: 1979, *Nuovo Cimento* **2C** (4), 421.
King, J.: 1989, *Interplanetary Medium Data Book NSSCD / WDC-A-R@S89-17*, Goddard Space Flight Center, Greenbelt, Maryland.

King, J. and Papitashvili, N. E.: 1994, *Interplanetary Medium Data Book NSSCD/WDC-A-R@S94-08*, Goddard Space Flight Center, Greenbelt, Maryland.
Legrand, J. P. and Simon, P. A.: 1981, *Solar Phys.* **70**, 173.
Lindblad, B. A.: 1981, *Solar Phys.* **74**, 187.
Lindblad, B. A. and Lundstedt, H.: 1981, *Solar Phys.* **74**, 197.
Marmatsouri, L., Vassilaki, A., Petropoulos, B., and Mavromichalaki, H.: 1995, *Adv. Space Res.* **16** (9), 245.
Mathews, J. and Papitashvili, N.: 1998, NSSDC OMNIWEB Data Explorer Results WWW Document (http://nssdc.gsfc.nasa.gov/omniweb/form/dx. html).
Mavromichalaki, H., Belehaki, A., and Rafios, X.: 1998, *Astron. Astrophys.* **330**, 764.
Mavromichalaki, H., Vassilaki, A., and Marmatsouri, E.: 1988, *Solar Phys.* **115**, 345.
Mavromichalaki, H., Belehaki, A., Rafios, X., and Tsagouri, I.: 1997, *Astrophys. Space Sci.* **246**, 7.
Rangarajan, G. K. and Mavromichalaki, H.: 1989, *Solar Phys.* **122**, 187.
Simon, P. A. and Legrand, J. P.: 1992, *Solar Phys.* **41**, 391.
Storini, M.: 1995, *Adv. Space Res.* **16** (9), 51.
Storini, M. and Felici, A.: 1994, *Nuovo Cimento* **170**, 697.
Storini, M. and Pase, S.: 1995, *STEP GBRSC News, Special Issue* **5**, 255.
Storini, M. and Sýkora, J.: 1997, *Solar Phys.* **176**, 417.
Storini, M., Pase, S., Sýkora, J., and Parisi, M.: 1997, *Solar Phys.* **172**, 317.
Swinson, D., Koyama, H., and Saito, T.: 1986, *Solar Phys.* **106**, 35.
Toptygin, I. N.: 1985, *Cosmic Rays in Interplanetary Magnetic Fields*, D. Reidel Publ. Co., Dordrecht, Holland.
Venkatesan, D., Shukla, A. K., and Agrawal, S. P.: 1982, *Solar Phys.* **81**, 375.
Xanthakis, J., Mavromichalaki, H., Tritakis, V., and Petropoulos, B.: 1994, in V. Rušin, P. Heinzel, and J. C. Vial (eds.), *Solar Coronal Structures*, p. 147.